

Design Strategy of Quantum Dot Thin-Film Solar Cells

Taewan Kim, Seyeong Lim, Sunhee Yun, Sohee Jeong,* Taiho Park,* and Jongmin Choi*

Quantum dots (QDs) are emerging photovoltaic materials that display exclusive characteristics that can be adjusted through modification of their size and surface chemistry. However, designing a QD-based optoelectronic device requires specialized approaches compared with designing conventional bulk-based solar cells. In this paper, design considerations for QD thin-film solar cells are introduced from two different viewpoints: optics and electrics. The confined energy level of QDs contributes to the adjustment of their band alignment, enabling their absorption characteristics to be adapted to a specific device purpose. However, the materials selected for this energy adjustment can increase the light loss induced by interface reflection. Thus, management of the light path is important for optical QD solar cell design, whereas surface modification is a crucial issue for the electrical design of QD solar cells. QD thin-film solar cell architectures are fabricated as a heterojunction today, and ligand exchange provides suitable doping states and enhanced carrier transfer for the junction. Lastly, the stability issues and methods on QD thin-film solar cells are surveyed. Through these strategies, a QD solar cell study can provide valuable insights for future-oriented solar cell technology.

1. Introduction

Quantum dots (QDs) are important materials in solar cell research because they enable investigators to push the limits of conventional photovoltaics (PVs).^[1] For example, the controllable energy levels of QDs have enabled a new route to fabricate solar cells that absorb from the ultraviolet to the infrared range, which can make high-efficiency tandem solar cells or transparent PVs feasible.^[2–5] Moreover, QD synthesis technologies

enable the derivation of new materials with a tailored bandgap for nontoxic solar cell.^[6,7] Meanwhile, QDs are the most potent materials that can overcome the Shockley–Queisser (S-Q) limit, the p-n junction limit of conventional solar cells, with a single material. The thermal energy loss of photons in a solar cell is reduced by energy conversion management methods such as carrier multiplication, up- and down-conversions, and hot carriers.^[1] Numerous researchers have been focusing on using QDs to realize such new-generation solar cell structures.

QD-sensitized solar cells exploit the distinct optical properties of QDs. Compared with conventional dye-sensitized solar cells, QD-sensitized solar cells have an adjustable band energy with a theoretically higher efficiency limit. Since 2006, when efficiencies less than 1% were reported, QD-sensitized solar cells have shown remarkably high growth rates.^[8]


In addition, QD-sensitized solar cells are well suited for the incorporation of environmentally friendly materials that exhibit excellent electrical properties but have not been previously used into solar cells because of their inadequate bandgap.^[9,10] However, QD-sensitized solar cells have similar problems as dye-sensitized solar cells. Specifically, poor device stability arising from the liquid electrolyte and limited interdot carrier mobility resulting from an excessively long ligand demonstrate a distinct need for the further development of materials and device structures.^[11]

QD thin-film solar cells are a good option to solve the aforementioned problems. Unlike QD-sensitized solar cell structures that rely on diffusion and tunneling at the interface for carrier transport because of poor conductivity of the QD, the QD thin-film solar cells have a driving force to separate and transport the carriers with band bending, resulting in sufficient mobility to make conducting film.^[12] **Figure 1** describes PbS QD thin-film solar cell structure. PbS QD active layer converts light into free carrier and each of the transport layers move the electron and hole, respectively. The energy diagram of each layer should be designed to match the absorption of light and the transfer of electric charges, especially the layer in which light enters is mainly transparent metal oxide having large bandgap. In addition, the device stability based on the thin-film structure is normally much higher than that of QD-sensitized solar cells because the cells are all-solid-state cells. Lastly, fabrication of each layer in QD thin-film solar cells is based on solution process, leading to excellent price competitiveness.^[13] Despite being developed

Dr. T. Kim, S. Lim, S. Yun, Prof. T. Park
Chemical Engineering
Pohang University of Science and Technology
Pohang 37673, Republic of Korea
E-mail: taihopark@postech.ac.kr

Dr. T. Kim, Prof. S. Jeong
Department of Energy Science and Center for Artificial Atoms
Sungkyunkwan University
Suwon 16419, Republic of Korea
E-mail: s.jeong@skku.edu

Prof. J. Choi
Energy Science & Engineering
Daegu Gyeongbuk Institute of Science and Technology
Daegu 42988, Republic of Korea
E-mail: whdals1062@dgist.ac.kr

 The ORCID identification number(s) for the author(s) of this article can be found under <https://doi.org/10.1002/sml.202002460>.

DOI: 10.1002/sml.202002460

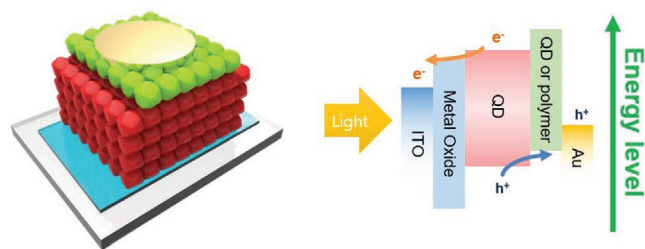


Figure 1. Basic structure and energy diagram of PbS QD solar cell.

concurrently with QD-sensitive solar cells, however, QD thin-film solar cells are less efficient because of the poor conductivity of QD film at the time.^[14] The efficiency of the devices began to increase after advances in the synthesis and surface chemistry of QDs, along with the development of new device structure. The mobility of QDs was dramatically improved when the interdot distance was shortened through the adoption of short ligands such as organic ligands with a small number of carbons or halide atomic ligands.^[15] Moreover, the modification of surface dipoles by doping led to a structural evolution from simple Schottky solar cells to heterojunction solar cells.^[12] Recent progress in QD thin-film solar cells has focused on surface modification of QDs because the main deficient device characteristic that remains to overcome is the surface trapping of QDs.^[3,16] Furthermore, several device designs have been proposed to optimize the light path, effective carrier transport, and stability of the devices.

Herein, we present a detailed design strategy for QD thin-film solar cell structures. In the optical design section, we survey the optical properties of QDs and what we consider important for solar cell structures from the viewpoint of optics. In addition, we discuss why an adjustment of the effective light path is needed in QD thin-film solar cells. In the electrical design section, we review the carrier dynamics and energy alignment necessary for QDs to provide high-efficiency QD thin-film solar cells. Third, we discuss the stability issue and related research necessary to approach commercialization. Despite the high stability of devices with an inorganic-based structure, the operando stability of QD thin-film solar cells in air and under illumination conditions should be carefully considered. Lastly, we provide recent approaches for eco-friendly QD solar cells. AgBiS₂ nanocrystal and III-V QDs were introduced as the most emerging materials. Here, we do not cover perovskite QD solar cell because most of the characteristics and weakness overlap with bulk perovskite, even though perovskite QD solar cells reported higher efficiency than other QD PVs.

2. Optical Design for QD PVs

The quantum confinement effect is an important concept for defining and understanding QDs. If nanoparticles are smaller than their exciton Bohr radius, the exciton is confined in zero-dimensional space and they exhibit quantized energy levels. Thus, the bandgap increases with decreasing particle size, which can affect the band structure and the absorption coefficient of materials. For example, a confined Si film has been reported to exhibit a shift in its band structure from an indirect to a direct bandgap.^[17] These unique features should be

considered to maximize the absorption of the target range of light to build solar cell.

In addition, the effective light path in QD thin-film solar cells is an important consideration in the structural optical design of a device. Because light reflection occurs at the interfaces of devices, minimizing the injected light reflection and maximizing the inner light reflection are important. In particular, a high reflective index of QDs for controlling the energy level can provide high Fresnel reflection at the interfaces, which is the main cause of light loss in QD solar cells.^[18] In this section, we discuss how optical properties of QDs are utilized to design QD thin-film solar cells.

2.1. Tunable Absorption of QDs by Confined Energy Level

Specifying the wavelength of light to be absorbed is the first step of designing QD solar cells. Because of the S-Q limit, the materials with bandgaps between 1 and 2 eV are commonly used as active materials for solar cells.^[19] However, QD solar cells offers a wider choice of materials compared with other solar cells based on bulk materials. Through the quantum confinement effect, the bandgap of QDs can be adjusted higher than that of original materials. That is, materials with a bandgap smaller than 1 eV can be used to fabricate the solar cells with a high S-Q efficiency limit. **Figure 2a** shows the spectral range of widely studied QDs.^[20] Notably, however, the range of bandgaps that can be adjusted is limited by the exciton Bohr radius of the materials. If nanoparticles smaller than their exciton Bohr radius cannot be synthesized, then their bandgap cannot be adjusted. Therefore, a large exciton Bohr radius and a large dielectric constant are preferred to enable strong quantum confinement effect. This is the reason why recent QD researches are mainly focused on heavy-metal compounds such as PbS and CdSe, or interested in covalent-bond materials such as InP and InAs.

Moreover, QDs can be a good alternative to other infrared-absorbing materials because of the tunability of their energy band.^[21–23] Basically, infrared-absorbing semiconductors should have a large lattice constant or large relative permittivity because the binding force between electrons and holes contributes to their bandgap.^[24,25] Thus, conventional infrared absorbers such as PbS, PbSe, HgCdTe, InSb, and InGaAs usually contain heavy metals or covalent bonds. These materials have a fixed bandgap, rendering them unsuitable to meet the target wavelength in many cases. For example, materials for absorbing/detecting wavelength of 1550 nm attract intensive attention because the light with this wavelength displays the best transmission in the fibers used in optical communication system. QDs can achieve such specific properties.^[26]

In the last few years, lead chalcogenide QDs have attracted widespread attention because of their excellent optical properties and size-tunable synthesis methods.^[27,28] For example, Pan et al. reported that the size of PbS QDs can be varied from 2 to 16 nm, resulting in bandgaps of 1.8 to 0.5 eV.^[29] Following the development of methods to enhance the conductivity of QD films through short-ligand exchange, PbS QDs have begun to be used for solar cell research in earnest. In the case of single active cells, PbS QDs with excitonic absorption peaks at wavelengths as long as 950 nm have been used to fabricate solar

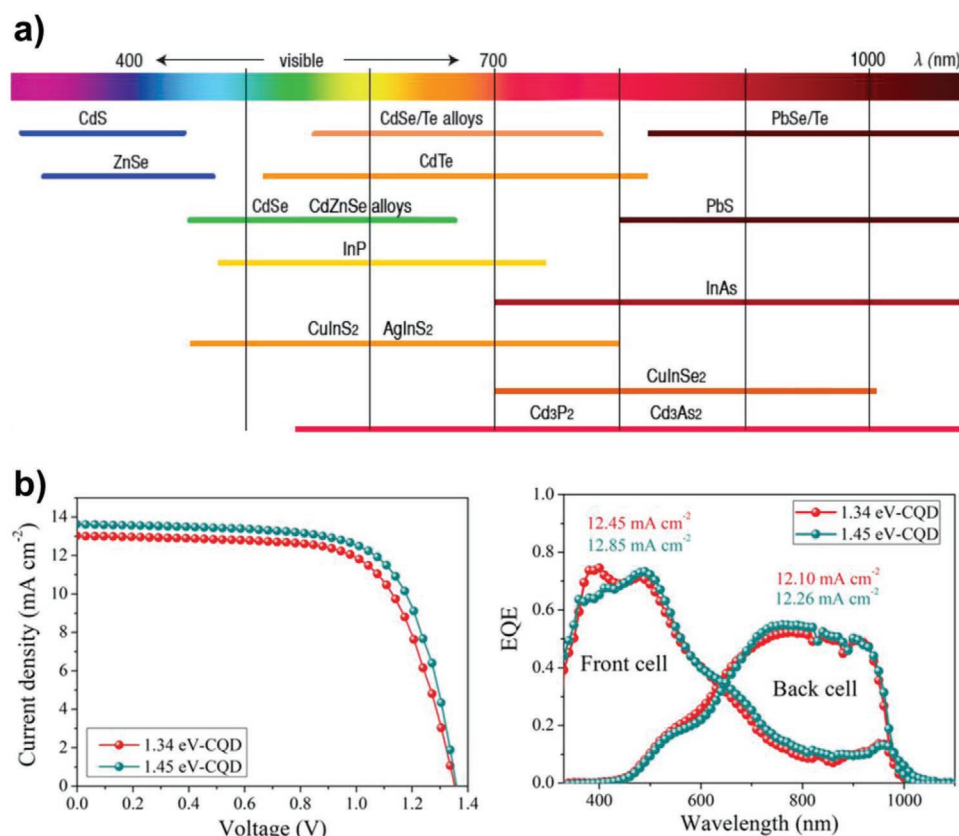


Figure 2. a) Emission spectrum of common binary and ternary QDs. Reproduced with permission.^[20] Copyright 2016, American Chemical Society. b) Current density–voltage curve and external quantum efficiency of polymer-PbS QD tandem devices. Reproduced with permission.^[31] Copyright 2020, Wiley-VCH.

cells with the best performance since the first depleted hetero-junction solar cell architecture was proposed.^[12,30] Except for the recently developed perovskite QDs, the most widely reported and most certified QD solar cells have been based on PbS QDs.

Furthermore, PbS QDs for tandem cells and photodetectors to absorb infrared light have attracted great attention because of their advantages of high stability, an adjustable bandgap, a solution-based fabrication process, and compatibility with soft electronic applications.^[2,21] By converting extra wavelength region via adjusted bandgap of QDs, the efficiency of other existing solar cells can be improved. Especially, QD active layer that can absorb visible and infrared light are useful in the fabrication of tandem structure with perovskite solar cells, organic solar cells, or even another QD solar cells that mainly absorb 800 nm or less. For example, Aqoma et al. reported organic-PbS QD tandem solar cells showing 12% of power conversion efficiency (PCE) recently (Figure 2b).^[31] We organized recent tandem solar cell development in Table 1.^[31–38]

2.2. Optical Architecture Design in Thin-Film QD Solar Cells

Although thicker QD films have an advantage in light absorption than thinner films because of Beer's law, the active layer of solar cells cannot be increased infinitely because the current density depends on the photocurrent and collection efficiency.

Excessively thick films cannot deliver generated carriers. Thus, despite the higher absorption coefficient of PbS and other QDs, the photocurrent and current density of QD thin-film solar cells are lower than those of Si wafer solar cells because of shorter carrier transport distance in the QD layer. In particular, the current loss at long wavelengths is critical because of the low absorption index in this region. In this section, we discuss the effective management of light path to increase the photocurrent of devices.

Light path management is the most common method to increase the performance of parallel-junction-based solar cells. The effective light path on solar cell structures has been improved in cases of PVs with silicon,^[39,40] cadmium telluride,^[41] copper indium gallium diselenide,^[42] perovskite,^[43] and other organic materials. In particular, PbS has a higher refractive index than other emerging materials such as organics and ^[44] perovskites,^[45] among other materials.^[46,47] The origin of the high refractive index of PbS QDs is unclear; however, a smaller bandgap of the PbS QD compared with those of other bulk materials may derive this high refractive index.^[48] This large dielectric constant provides a high refractive index difference between ZnO and PbS QDs, leading to superb Fresnel reflection in QD thin-film solar cell. The excessive optical interference effect produced by Fresnel reflection not only shortens the effective light path but also limits the thickness of the QD active layer according to our recent study.^[18] Therefore, numerous researchers have attempted

Table 1. Recent QD based tandem solar cells.

Year	Structure	V_{OC} [V]	J_{SC} [mA cm ⁻²]	FF	PCE [%]	Ref.
2015	PbS QD	0.57	14.4	0.44	3.6	[32]
	PTB7:PC ₇₁ BM	0.75	16.1	0.64	7.7	
	Tandem	1.25	6.1	0.69	5.3	
2017	PbS QD	0.50	15.5	0.65	5.0	[33]
	PTB7-Th:PC ₇₁ BM	0.79	15.9	0.70	8.3	
	Tandem	1.25	9.9	0.74	9.1	
2017	PbS QD	0.58	13.7	0.66	5.3	[34]
	PbS QD	0.58	22.3	0.64	8.3	
	Tandem	1.13	12.3	0.64	8.9	
2018	PTB7:PC ₆₁ BM	0.74	17.4	0.61	7.9	[35]
	PbS QD	0.58	21.8	0.55	7.0	
	Tandem	1.31	12.5	0.57	9.3	
2018	PbS QD	0.55	12.9	0.67	4.8	[36]
	Perovskite	1.11	17.6	0.70	13.6	
	Tandem	1.66	8.9	0.75	11.0	
2018	PbS QD	0.68	14.5	0.62	6.1	[37]
	PbS QD	0.50	23.7	0.60	7.1	
	Tandem	1.12	12.4	0.59	8.2	
2019	PbS QD	0.66	12.8	0.64	5.4	[38]
	PbS QD	0.49	23.8	0.58	6.7	
	Tandem	1.02	11.7	0.55	7.1	
2020	PbS QD	0.67	17.1	0.70	8.2	[31]
	PTB7:PC ₆₁ BM	0.69	24.1	0.66	11.0	
	Tandem	1.35	13.0	0.68	12.0	

V_{OC} , open-circuit voltage; J_{SC} , short-circuit current; FF, fill-factor; PCE, power conversion efficiency.

improve the effective light path using optical structure design at the interfaces or the end of the devices. **Figure 3a** displays how optical architecture can improve light absorption in QD solar cells.^[49]

The high reflection and interference effect depend mainly on the different refractive index and parallel interface structures. Thus, most strategies of optical management rely on removing the refractive index gap through the use of other sublayers or on tuning the light path through structural control. The basic principle for improving the amount of absorbed light is maximizing incoming light and minimizing outgoing light. Zhang et al. deposited a thin TeO₂ antireflection coating onto the Au electrode of transparent PbS QD solar cells.^[50] Using measurements of actual devices and theoretical simulations, they found that optical losses were decreased, reporting a transmittance of 20.4% and a PCE of 7.3%. Lavelle et al. used pyramid-patterned electrode structuring to induce a light-trapping effect (Figure 3b).^[51] These light management approaches are particularly effective when the interference effect is removed or light is concentrated on an active-layer region with a high carrier collection efficiency. Kim et al. reported that nanostructured ZnO/PbS QD interfaces can provide decreased interference and concentrated light, as revealed by measured solar cell data and computer simulation.^[18]

The light-scattering effect is another widely known method to achieve greater light absorption in various thin-film solar cells.^[52–54] Wang et al. fabricated enhanced PbS QD solar cells with ZnO nanowire to improve their absorption in the near-infrared region.^[55] More recently, Cho et al. reported the light-trapping effect of different array shapes in PbS QD-, organic-, and perovskite-based solar cells.^[49] In addition, Chen et al. and our group independently showed that metal nanoparticles in the light path enhanced the light-scattering effect in PbS QD solar cells, improving their light-harvesting ability (Figure 3c).^[56,57]

3. Electrical Design for QD PVs

The electrical properties of QDs are the core issue in fabricating high-performance PVs. Because of the high surface-area-to-volume ratio and interdot distance, carrier transport in QD films relies on surface modification and short-ligand treatments. Moreover, the energy state and Fermi level of QDs are also affected by the ligands. Through doping, carriers generated by photon energy can be extracted via band bending. These developments enable enhanced device architectures with improved active-layer thickness in thin-film QD solar cells.

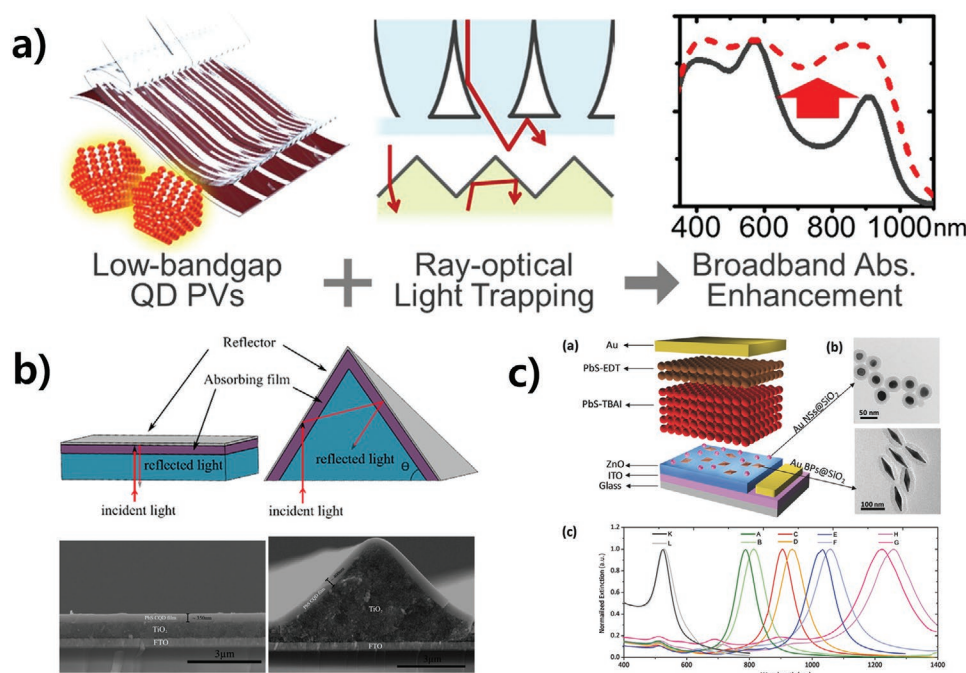


Figure 3. a) Scheme of effective light management and quantum efficiency enhancement of QD thin-film solar cells. Reproduced with permission.^[49] Copyright 2015, Springer Nature. b) Pyramid-patterned QD thin-film solar cell and its light-trapping. Reproduced with permission.^[51] Copyright 2015, American Chemical Society. c) Nanoparticle-induced QD thin-film solar cell with light-scattering effect. Reproduced with permission.^[56] Copyright 2015, Wiley-VCH.

Furthermore, surface modification of QDs is a major approach to controlling trap density and energy alignment of the devices. Unfavorable surface passivation by adatoms, dangling bonds, and defects reveal various in-gap states that induce fast recombination of electrons and holes. In addition, the dipole moment produced by the surrounding ligand provides energy shifting of the QDs. Thus, a homogeneous QD film with a graded energy state enables effective carrier collection in QD thin-film solar cells. Therefore, surface chemistry modification is the main strategy used to enhance the efficiency of solar cells.

3.1. Basic Device Architecture for Carrier Transport in QD PVs

To achieve thin-film structure solar cells, the carrier mobility and interdot charge transfer are critical properties because the generated carriers must move at least hundreds of nanometers in QD films.^[58] The major determinant of fast carrier transport is interdot distance. Liu et al. reported that the mobility in PbSe nanocrystalline solids decreases exponentially with regards to the length of dithiol ligands and QD diameter (Figure 4a).^[59] Thus, treatment with short ligands such as 3-mercaptopropionic acid (MPA), 1,2-ethanedithiol (EDT), or with atomic halide ligands is essential to fabricating junction-type thin-film QD solar cells.^[15,60,61] In 2008, Luther et al. reported Schottky solar cells based on EDT-treated PbSe QDs between Indium-doped tin oxide (ITO) and a metal electrode.^[14] Atomic ligand treatment based on an organic ammonium halide salt was later introduced by Tang et al.^[62] This atomic ligand results in a much shorter interdot distance with improved mobilities compared with short organic ligands.

Recent papers on PbS QD solar cells have shown that iodide ligand is most effective for passivating PbS QD with high mobility.^[3,63] However, this high mobility is not the only reason for using iodide in PbS QDs. More importantly, the doping state of QDs must be controlled to fabricate high-performance QD solar cells and the halide passivation of QDs must be suitable for p-n junction design.^[12,64,65] In case of Si, high doping results in a long diffusion length with improved mobility, enabling Si solar cells to have a thickness greater than hundreds micrometers. However, the diffusion length produced by QDs is currently on the order of $10^{-2} \text{ cm}^2 \text{ V}^{-1} \text{ s}^{-1}$ today. Thus, the carrier transport of QD PVs mainly depends on the band bending produced by hetero p-n junction.

Pattantyus-Abraham et al. summarized the advantages of depleted heterojunction QD solar cell produced by n-type metal oxide and p-type QD films compared to Schottky and sensitized cell architectures (Figure 4b).^[12] First, the absorption of light with high photon energy begins at the p-n junction region, which provides almost 100% collection efficiency. Because of the absorption coefficient shape of QDs, the carrier generation rate decreases with increasing of QD thickness.^[66] Therefore, most carrier generation occurs on the illuminated side. Second, less Fermi-level pinning occurs in the junction solar cell, resulting in a smaller open-circuit voltage (V_{OC}) deficit. Third, the deep valance level of the metal oxide prohibits the charge carrier recombination. Through this structural design, the active layer thickness of the QD solar cells could be increased from 100 nm or less to 300 to 400 nm or more.

Iodide-treated PbS QDs provide an adequate intrinsic or p-type doping state for these p-n junction structures. However, early analyses of doping level of PbS QDs were unclear

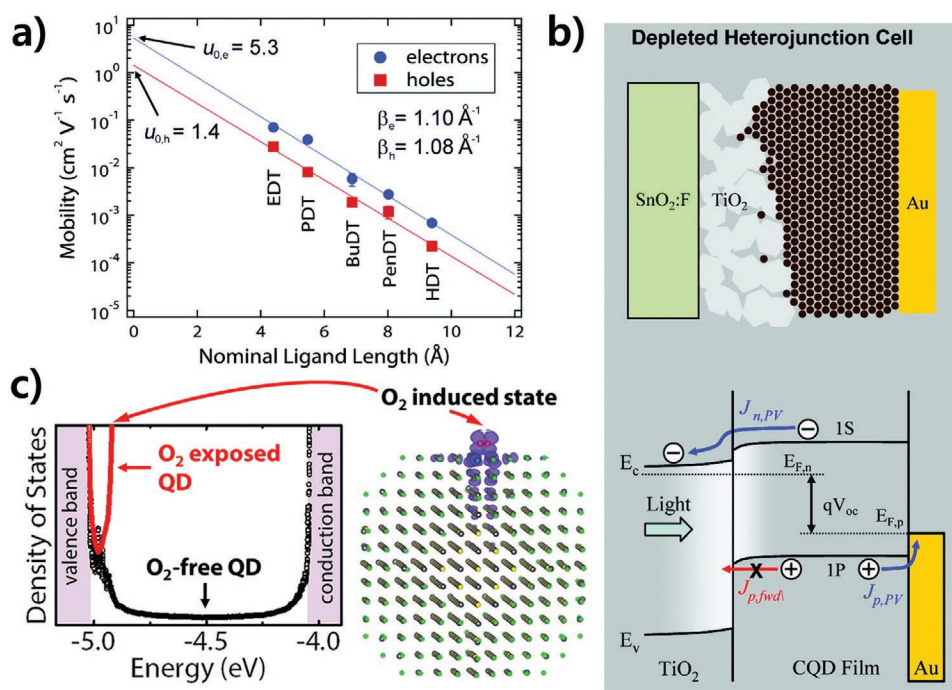


Figure 4. a) Linear proportional relationship between length of dithiol-ligand and carrier mobility. Reproduced with permission.^[59] Copyright 2010, American Chemical Society. b) Heterojunction QD solar cell structure and band bending produced by depletion width. Reproduced with permission.^[12] Copyright 2010, American Chemical Society. c) Remote oxygen doping effect on PbS QD. Reproduced with permission.^[68] Copyright 2015, American Chemical Society.

because of the remote oxygen doping effect of PbS QD surfaces;^[67] iodide-treated PbS QDs were consequently expected to exhibit n-type doping. Like the doping state of other common semiconducting materials, that of PbS QDs was commonly obtained using ultraviolet photoelectron spectroscopy. However, reported work by Zhang et al. suggested that the doping state of PbS QDs can vary with oxygen condition.^[68] Figure 4c shows that reversible oxygen attachment onto (100) facets of PbS QDs generates a p-doping energy state. These p-type iodide-treated PbS QD conducting films can exhibit a longer depletion width, representing enhanced active-layers thickness.^[69] Moreover, Chuang et al. treated PbS QD layer with EDT onto iodide-treated PbS QD layer to induce interfacial band bending.^[70] The absorption of the EDT-treated PbS QD layer was even lower than that of the iodide-treated layer; band adjustment enhanced the efficiency and stability of PbS QD solar cells.^[70,71]

Most recently, several attempts to increase carrier diffusion length of QDs by using homo- and heterojunction composite structure has drawn attention. In 2020, Choi et al. suggested

PbS QD homojunction by different doped PbS QD, similar to donor–acceptor heterojunction of organic solar cells. By improved diffusion length, thickness of PbS QD active layer achieved 550 nm showing 30 mA cm^{-2} short-circuit current (J_{sc}) and 13.3% PCE.^[72] Moreover, perovskite-treated PbS QD solid engineering continuously updated the maximum PCE of PbS QD solar cells. The heteroepitaxial growth of perovskite on PbS QDs with appropriate lattice parameter matching provides enhanced mobility and interdot packing to QD solid film.^[73,74] Latest perovskite monolayer bridged PbS QD solar cell fulfilled 13.8% record PCE.^[74] Table 2 shows the representative efficiency of each device structure in PbS QD solar cell.^[63,70,74–76]

3.2. Energy Level Tuning of QDs and Its Application on PV

The energy alignment of constituent materials is the other main determinant of solar cell design. Specifically, the surface chemistry of QDs drives several pros and cons in QD solar cells

Table 2. Representative PbS QD solar cells with various structures.

Year	Structure	V_{oc} [V]	J_{sc} [mA cm^{-2}]	FF	PCE [%]	Ref.
2012	FTO/ $\text{TiO}_2/\text{ZnO}/\text{PbS QD}/\text{MoOx}/\text{Au}/\text{Ag}$	0.59	21.8	0.58	7.4	[75]
2014	ITO/ $\text{ZnO}/\text{PbS QD}/\text{PbS-EDT}/\text{Au}$	0.55	24.2	0.64	8.6	[70]
2016	ITO/ $\text{ZnO}/\text{PbS QD ink}/\text{PbS-EDT}/\text{Au}$	0.61	27.2	0.68	11.3	[76]
2018	ITO/ $\text{ZnO}/\text{PbS QD ink-PbI}_2/\text{PbS-EDT}/\text{Au}$	0.65	29.0	0.64	12.0	[63]
2020	ITO/ $\text{ZnO}/\text{PbS QD ink-perovskite}/\text{PbS-EDT}/\text{Au}$	0.65	30.0	0.71	13.8	[74]

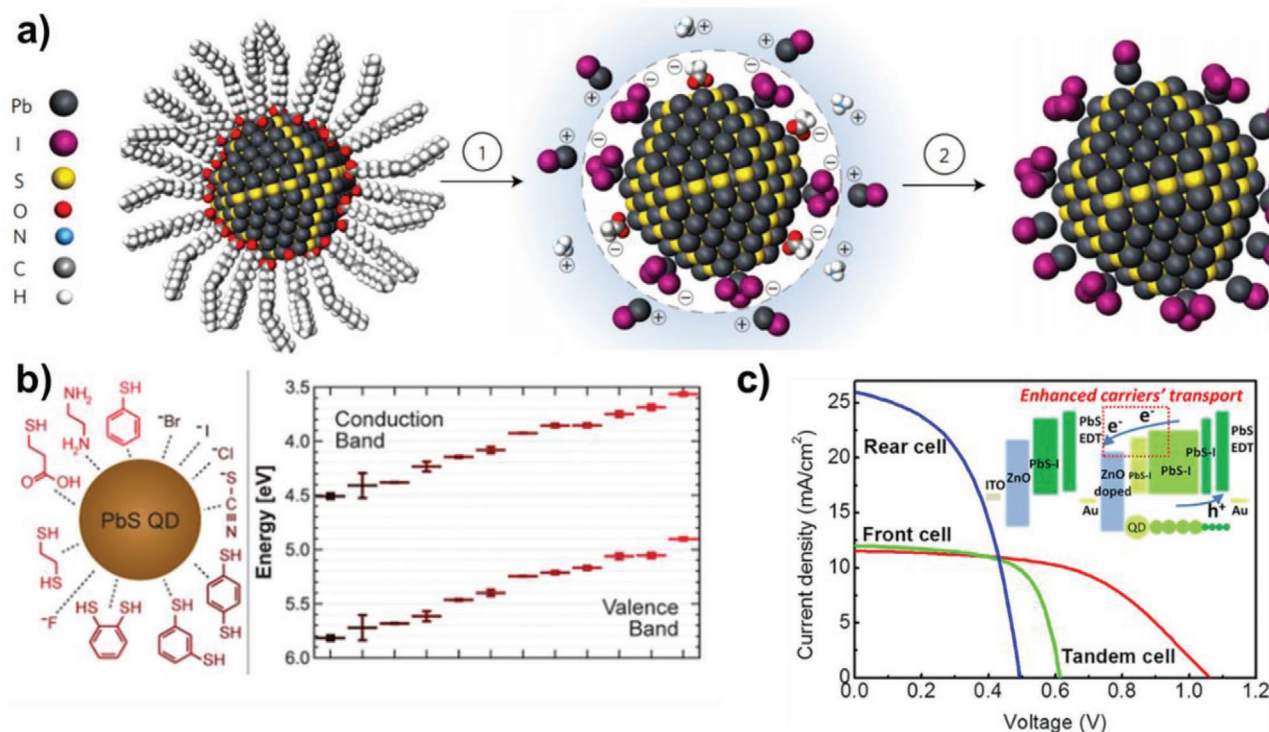


Figure 5. a) Solution-phase ligand exchange with metal halide precursors. Reproduced with permission.^[76] Copyright 2016, Springer Nature. b) Various ligand effect on energy level of PbS QD. Reproduced with permission.^[87] Copyright 2014, American Chemical Society. c) Band align modification for high efficient tandem cells. Reproduced with permission.^[89] Copyright 2019, American Chemical Society.

because of the large surface-area-to-volume ratio of QDs. For example, the high trap density produced by surface dangling bonds is a chronic problem in QD optoelectronics, including solar cells and LEDs. Researchers have developed various strategies to observe and modify the surface chemistry of QDs. Choi et al. showed that PbS QDs have a different shape and facet ratio with respect to the QD radius, suggesting the need for customized surface adjustment strategies.^[16] In particular, 3–4 nm of PbS QDs, which exhibit a bandgap suitable for solar cells, consist of a large area of (111) facets with numerous Pb cations on the PbS QD surfaces. Thus, controlling of (111) facet plays a key role in passivating PbS QDs.

As previously mentioned, ligand exchange to obtain high-mobility QD films is important when fabricating the devices. However, solid-state ligand exchange, which is usually carried out using layer-by-layer (LBL) process, has been reported to lead to films contaminated with remaining organics compounds as well as to the waste of QDs.^[77] Carey et al. reported that the remaining organics can inhibit carrier collection and increase recombination in PbS QD solar cells.^[78] More recently, Liu et al. developed a solution-phase ligand exchange process for PbS QDs with oleate ligands.^[76] Figure 5a displays the scheme of the solution-phase ligand exchange with halide ligands. Compared with the LBL method, this hybrid QD ink production provides greater ligand passivation and improved performance in PbS QD solar cells.

Hydroxylation is another common issue related to PbS QD passivation. Zherebetsky et al. reported that (111)-facet hydroxylation occurs during synthesis of PbS QDs.^[79]

Despite the hydroxyl group (OH) ligands stabilizing the (111) facet, this bonding is the origin of traps in PbS QD energy state after ligand exchanges. Specifically, OH ligand binding inhibits the binding of other short ligands such as thiolate and iodide.^[80] Thus, Wang et al. recently described a new method of synthesizing PbS QDs for optoelectric devices that involves replacing the PbO precursor with Pb acetate.^[81] Nevertheless, this OH ligand passivation is a critical problem because not only synthesis but also the purification steps lead to hydroxylation.^[81–83] The polarity-based purification with methanol solvent is essential for removing the byproduct generated during PbS QD synthesis;^[84] however, this protic solvent induces OH ligand passivation at the QD surfaces. Therefore, numerous researchers have tried to remove hydroxyl group to obtain high performance of PbS CQD solar cells.^[79–81,85] Gu et al. reported that iodide-passivated PbS QDs have numerous unremoved OH ligands, and additional MPA treatment can exchange the OH ligands to MPA ligands, reducing band tail and trap density of the PbS QDs.^[65]

Moreover, energy alignment of QD layers, as controlled by different ligand dipole or various QD size, is another route to enhance performance of QD solar cells. Kroupa et al. have reported that the conduction- and valance-band shift of PbS QDs is proportional to the dipole moment of ligands.^[86] In the present paper, the dipole moment and functional group of ligands are suggested to be a critical parameter influencing the band-edge shift. The contribution of the short ligand effect to conducting PbS QD films was investigated by Brown et al. (Figure 5b)^[87] For example, halide-treated PbS QDs represent

deeper band edges, whereas thiol ligands contribute to shallower band edges. The results suggest that the difference in band-edge shift is decided by the total dipole, which is the sum of QD/ligand interface dipoles and intrinsic ligand dipoles. This controllable band alignment is useful in the design of more effective band structure. These studies have been effectively applied to build suitable band designs in junction-type PbS QD solar cells.^[88] This band modification also occurs using size-controlled QDs. Recently, Gao et al. investigated the graded band structures of PbS QDs to obtain an appropriate junction for use in tandem devices (Figure 5c).^[89] This energy alignment design reinforces effective carrier collection in QD solar cells.

4. Stability Issue and Design for QD PVs

Solar cell design for stability is also an important subject in the QD PV industry. The device lifetime of QD thin-film solar cells mainly depends on the QDs themselves, which often consist of large surface area and organic–inorganic hybrid ligands. Even though most QDs reveal high crystalline based on high temperature-based synthesis, degraded surface of QDs detrimentally affect their size-dependent characteristics. For example, oxidized QDs shows optical blue-shift spectrum owing to reduction of effective volume.^[90] This surface degradation is usually produced by oxygen or water in the air condition and can be promoted by light and temperature.^[91] Further, trap states formed by harmed surface can decline device performance in long-term measurement.^[80] In this section, we discuss several reported achievements to improve stability issue in terms of QD materials and device design, respectively.

4.1. Stability Improvement via Synthesis and Surface Chemistry

Because QDs have various facets with different atom stoichiometry, ligand binding cannot passivate all of the QD surfaces equally. The Pb-chalcogenide QDs consist of (111) and (100) facets, both of which have stability issues. For example, oxygen attack at the (100) facet of a PbSe QD is a major oxidation mechanism that leads to energy trap states and a blue-shift effect.^[92] By contrast, the (111) facet is more well-capped by anion ligands because of its cation-rich surface state. However, unpassivated dangling bonds or hydroxylation during the synthesis and ligand exchange can also result in trap states. The first approach to enhancing the surface chemistry of PbS QDs is improving the synthesis method. The PbO precursor contributes to surface hydroxylation during PbS QD synthesis, and this hydroxylation leads to an in-gap trap state that reduces the efficiency of solar cells.^[79,80,85] Wang et al. developed a new synthesis method using Pb acetate to decrease the abundance of attached hydroxyl group.^[93] The air- and photostability of the solar cell was improved compared with that of conventional PbS QD solar cells synthesized with lead oxide. Moreover, in situ halide passivation during the PbS QD synthesis has been reported by Zhang et al. (Figure 6a).^[94] According to their paper, the photoluminescence and photostability increase when lead halide is used as lead source.

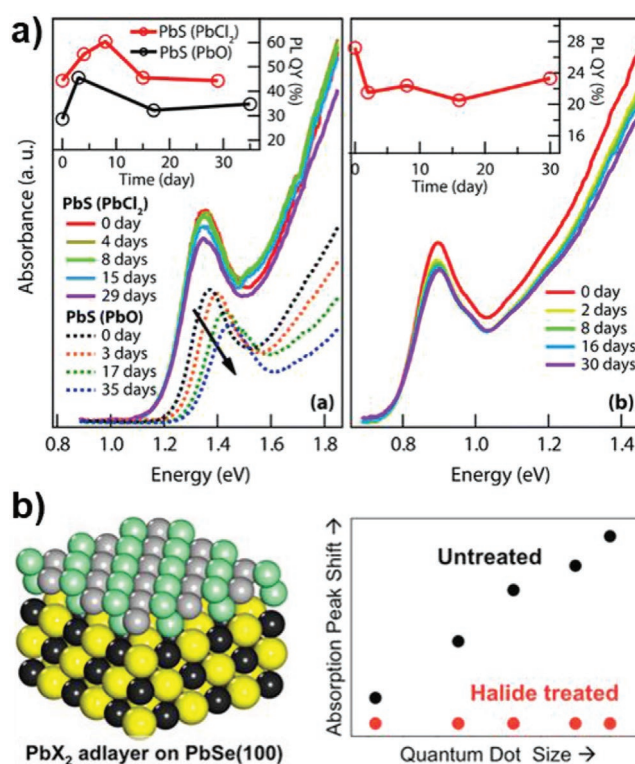


Figure 6. a) Absorption and PLQY of PbS and PbSe QDs with in-situ halide passivation synthesis. Reproduced with permission.^[94] Copyright 2014, American Chemical Society. b) Surface passivation by lead halide adlayer on PbSe and its absorption peak shift over time progress. Reproduced with permission.^[97] Copyright 2014, American Chemical Society.

Another step in enhancing the stability for PV device applications is ligand exchange. In the QD luminescence field, core–shell structure or long ligands are typically introduced as an after-treatment to block molecule access, enhancing the stability of the QDs.^[95] As previously mentioned, however, they are not suitable methods for fabricating solar cells because the interdot distance is too large for efficient transport of the generated carriers. Therefore, finding facets with high reactivity and devising strong binding ligands is the main strategy for QD PVs.

Ning et al. suggested that PbS QDs with various single halide ligands (Br[−], Cl[−], and I[−]) have different air stability because the large bulkiness of iodide atom inhibits oxygen adsorption.^[96] Moreover, Woo et al. reported a halide-based adlayer on PbSe QDs that improves their air stability dramatically because of passivation of the most reactive (100) facet.^[97] Figure 6b reveals a small absorption peak shift of lead halide-passivated PbSe QDs over time. More recently, Choi et al. reported surface modification of PbS QD in operando conditions using potassium iodide, which is oxidized before the formation of PbO.^[98]

4.2. Device Architecture Design for Stability of QD PVs

Here, we discuss additional layer and interface engineering routes to improve device stability. Before 2014, the QD active

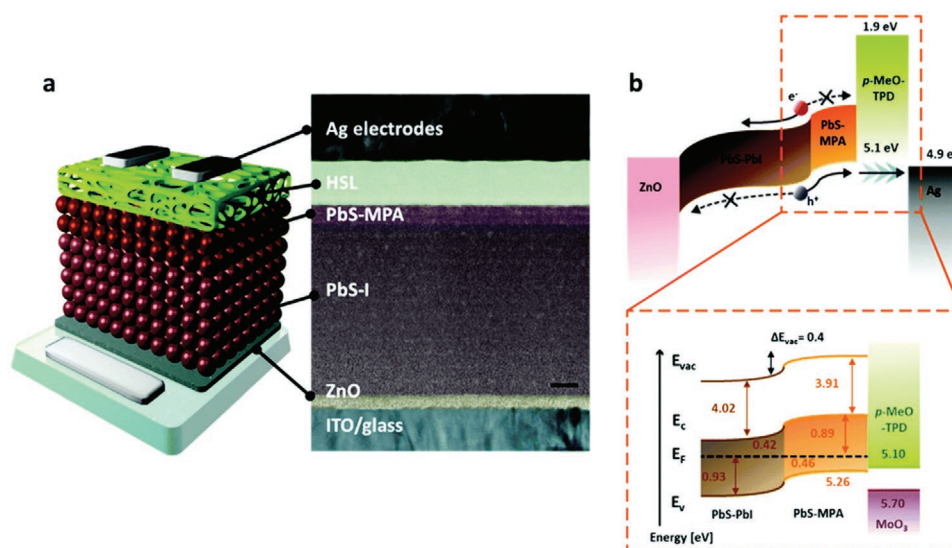


Figure 7. Structure and energy diagram of hydro/oxo-phobic hole selective layer (HSL) introduced PbS QD solar cell. Reproduced with permission.^[103] Copyright 2018, Royal Society of Chemistry.

layer in solar cells directly contacted unstable materials such as LiF or MoOx to transfer the carriers, leading to diminished performance over time.^[70,99,100] Chuang et al. first suggested an EDT-treated PbS QD layer as an alternative to other hole transport layer.^[70] The band alignment effect and exclusion of unstable matter provided a higher solar cell efficiency and device stability. Thus far, this solar cell structure with band alignment is a popular topic of papers related to PbS QD solar cells because of its excellent efficiency and stability.

Nevertheless, oxygen and moisture still penetrate through naked surfaces of the device. Likewise, in other optoelectronic devices with an unstable active layer such as a perovskite layer, the air or water blocking layer is effective for QD solar cells.^[101,102] For example, a hydrophobic graphdiyne film was introduced as a HTL and moisture-blocking layer in 2006.^[102] The long-term stability of the device was improved and recombination that occurred at the interface between the PbS–EDT layer and Au was reduced. More recently, Back et al. reported a hydro/oxophobic pore layer for PbS QD solar cells.^[103] The improved optical and electrical properties and stability of the device led to a PCE of 11.7%, and the device retained 90% of its PCE after 1 year (Figure 7).

5. Eco-Friendly Material Design for QD PVs

Wavelength targeting for photoconversion has been improved; however, most of the reported works have involved Pb-based materials. PV technologies are now moving forward to solar cells using eco-friendly materials.^[104] Pb- and Cd-free QDs with an adjustable bandgap and high stability are highly desirable for use in eco-friendly QD thin-film solar cells compared with polymers, perovskites, and other emerging materials. Herein, we discuss AgBiS₂ nanocrystals and III-V QDs as the most emerging eco-friendly solar cell materials.

5.1. AgBiS₂ Nanocrystal Solar Cells

The highest-performing eco-friendly QD thin-film solar cells is based on AgBiS₂ nanocrystals, displaying 6.2% efficiency with room for improvement.^[6] Colloidal AgBiS₂ nanocrystal has higher absorption coefficient compared to PbS QDs, enabling similar level of J_{SC} to PbS QDs even with a thickness of one-tenth. Further, in situ ambient synthetic process of AgBiS₂ nanocrystals was recently reported by the same group, enabling large-scale production of non-toxic solar cell materials.^[105] However, because of the difficulty of optical analysis resulting from a lack of photoluminescence and high polydispersity in size, surface structure, and composition, significant enhancement has not been reported since the initial paper.^[106] There have been several attempts to increase the homogeneity of AgBiS₂ nanocrystals size, but reported PCE values are still below 6%.^[107,108] In addition, carrier diffusion length of iodide-treated AgBiS₂ nanocrystal film is up to 60 nm due to the uncontrolled defect traps, limiting the thickness of active layer in solar cells.^[109]

5.2. III-V QD Solar Cells

Other emerging QDs for eco-friendly PVs are III-V QDs. The III-V QDs have high covalency, promising a large dielectric constant and large exciton Bohr radius. For example, InAs and InSb bulk materials have bandgaps of 0.35 and 0.23 eV with exciton Bohr radii of 34 and 65 nm, respectively. These suitable bandgaps and huge exciton Bohr radii enable a broad and tunable absorption range in visible to near IR light. Note that InP QD, one of the III-V with higher bulk bandgap, when used in solar cell, provides only around 1% efficiency due to inadequate bandgap and insufficient surface treatment.^[110,111] Nevertheless, the development of III-V QDs for PVs faces numerous obstacles.^[112,113] First, there are numerous trap sites from intractable bonds and surfaces. For example, the high trap density of InAs

Table 3. Eco-friendly QD solar cells.

Year	Structure	V_{OC} [V]	J_{SC} [mA cm ⁻²]	FF	PCE [%]	Ref.
2016	ITO/ZnO/AgBiS ₂ NP/PTB7/MoO _x /Ag	0.45	22.1	0.63	6.31	[6]
2018	ITO/ZnO/In(Zn)P/MoO _x /Ag	0.468	6.7	0.37	1.17	[111]
2020	ITO/PEDOT:PSS/InP QD/ZnO/Al	0.35	3.3	0.36	0.41	[110]

QDs leads to poor diffusion of carriers and a short depletion width because the surface traps induce high n-type doping as well as recombination sites.^[7] In addition, synthetic methods for controlling oxidation and byproduct formation have not been established enough. Last, ligand exchange strategy was not much established in III-V QDs, mainly because of the lack of understanding atomistic details of III-V QD surfaces.^[114] The state-of-the-art performing fabrication process of InAs QD solid film reported to date is two-step surface treatment using NOBF₄ and short ligand.^[7] While excessive doping and trap density in the QD film should be controlled to serve as a major active layer, it is the first reported solar cell device fabricated at low temperature, below 100 °C. **Table 3** represents reported eco-friendly QD solar cells.^[6,110,111]

6. Conclusion

In summary, we have surveyed the optical and electrical properties and stability of QDs and customized solar cell design approaches. However, the most efficient QD thin-film solar cell is still less efficient than the solar cells composed of emerging materials such as organics and perovskites and those composed of other thin films and Si wafers.^[115] Therefore, which trait of QDs contributes to their shortfall of conversion efficiency and how to enhance today's design approaches should be investigated.

Numerous obstacles impede the advancement of future-oriented solar cell technology in thin-film QD solar cell research. First, the conductive film construction of eco-friendly QDs has rarely been studied. For example, the InAs QDs, which are representative III-V nontoxic QDs with a suitable bandgap for solar cells, have an excessively high n-doping concentration and trap density to be used in solar cells because of their ordinary surface chemistry.^[7] Thus, building an effective active-layer thickness of InAs QDs using heterojunction structures is effective. Furthermore, carrier transfer from the conduction band to a dark state in QDs results in a critical V_{OC} deficit issue in QD thin-film solar cells. Voznyy et al. have reported that packed and polydispersed PbS QDs exhibit a large Stokes shift that exceeds theoretical estimations.^[116] Thus, the V_{OC} of thin-film QD solar cells is reduced by this energy level being lower than its conduction band, leading to band tailing and limiting efficiency.^[117] This effect is commonly observed with other QDs, indicating that other QDs may have a similar problem with respect to incorporation into solar cells.

Currently, the most notable study to lead the study of QD thin-film solar cells is the hybrid junction active layer structure. The best efficiency of QD thin-film solar cells has always been achieved by electrical design and surface chemistry, meaning the low efficiency of QD thin-film solar cells

compared to Si solar cells is originated from the poor electrical characteristics of QD solid film. The recently reported perovskite-QD composite structure addresses difficult problems such as poor surface treatment and short diffusion length while taking advantage of the optical advantages of QDs.^[73,74] If this structure can be introduced into the current eco-friendly QDs, it will have great benefits in terms of efficiency, stability, and non-toxicity.

The development of the carrier transport layer specialized in QD PVs is important, too. Almost all current PbS QD solar cells rely on ZnO for electron transport, but even the reason is not clear. To date, the optical design of the ZnO interface may have increased current, but it has never achieved record efficiency due to its decreased electrical characteristics such as mobility or conductivity.^[118] Moreover, there are several reports that the PbS-EDT layer does not have low trap density and excellent carrier delivery compared to the iodide-treated PbS QD layer.^[118] The introduction of QD thin films through new ligand treatment may improve these problems more easily because the PV structure that consists of the same QD film can carry free carriers by p-n junction structure with minimal Fresnel reflection.

These problems are fundamentally rooted in a lack of knowledge of the synthesis mechanism and carrier transport process. Compared with their corresponding bulk materials, QDs can exhibit various sizes, shapes, dimensions, and crystal structures. Therefore, researchers should consider additional factors such as surface energy with a different facet and assorted reaction paths compared with bulk materials.^[119] Moreover, carrier transport at the nanoscale shows different tendencies compared with the predictions of classical physics, which mainly depends on surface ligands and the density-of-state of the materials.^[120] Without tailored synthesis and surface modification strategies for QDs, high carrier recombination and constrained carrier collection as well as poor material stability will remain cumbersome hurdles to the fabrication of commercial QD solar cells. Therefore, the need for a deep understanding of QD science continues to increase.

Acknowledgements

This work was supported by the NRF grant funded (2019M3D1A1078299, 2018R1A2A1A05079144, and 2020R1C1C1012256). This work was also supported by POSCO Science Fellowship of POSCO TJ Park Foundation.

Conflict of Interest

The authors declare no conflict of interest.

Keywords

electrics, optics, photovoltaic design, quantum dots, thin-film solar cells

Received: April 17, 2020

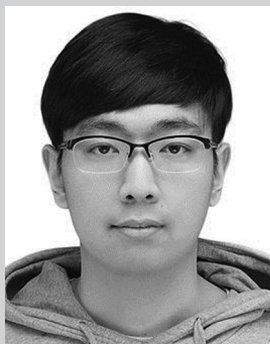
Revised: July 28, 2020

Published online: October 20, 2020

- [1] O. E. Semonin, J. M. Luther, M. C. Beard, *Mater. Today* **2012**, 15, 508.
- [2] D. Zhao, J. Huang, R. Qin, G. Yang, J. Yu, *Adv. Opt. Mater.* **2018**, 6, 1800979.
- [3] M. Yuan, M. Liu, E. H. Sargent, *Nat. Energy* **2016**, 1, 16016.
- [4] E. S. Arinze, B. Qiu, N. Palmquist, Y. Cheng, Y. Lin, G. Nyirjesy, G. Qian, S. M. Thon, *Opt. Express* **2017**, 25, A101.
- [5] S. E. Sofia, J. P. Mailoa, D. N. Weiss, B. J. Stanbery, T. Buonassisi, I. M. Peters, *Nat. Energy* **2018**, 3, 387.
- [6] M. Bernechea, N. C. Miller, G. Xercavins, D. So, A. Stavrinadis, G. Konstantatos, *Nat. Photonics* **2016**, 10, 521.
- [7] J. H. Song, H. Choi, H. T. Pham, S. Jeong, *Nat. Commun.* **2018**, 9, 4267.
- [8] Z. Pan, H. Rao, I. Mora-Seró, J. Bisquert, X. Zhong, *Chem. Soc. Rev.* **2018**, 47, 7659.
- [9] Z. Pan, I. Mora-Seró, Q. Shen, H. Zhang, Y. Li, K. Zhao, J. Wang, X. Zhong, J. Bisquert, *J. Am. Chem. Soc.* **2014**, 136, 9203.
- [10] C. C. Chang, J. K. Chen, C. P. Chen, C. H. Yang, J. Y. Chang, *ACS Appl. Mater. Interfaces* **2013**, 5, 11296.
- [11] J. H. Bang, P. V. Kamat, *ACS Nano* **2009**, 3, 1467.
- [12] A. G. Pattantyus-Abraham, I. J. Kramer, A. R. Barkhouse, X. Wang, G. Konstantatos, R. Debnath, L. Levina, I. Raabe, M. K. Nazeeruddin, M. Grätzel, E. H. Sargent, *ACS Nano* **2010**, 4, 3374.
- [13] J. Jean, J. Xiao, R. Nick, N. Moody, M. Nasilowski, M. Bawendi, V. Bulović, *Energy Environ. Sci.* **2018**, 11, 2295.
- [14] J. M. Luther, M. Law, M. C. Beard, Q. Song, M. O. Reese, R. J. Ellingson, A. J. Nozik, *Nano Lett.* **2008**, 8, 3488.
- [15] D. Bederak, D. M. Balazs, N. V. Sukharevskaya, A. G. Shulga, M. Abdu-Aguye, D. N. Dirin, M. V. Kovalenko, M. A. Loi, *ACS Appl. Nano Mater.* **2018**, 1, 6882.
- [16] H. Choi, J. H. Ko, Y. H. Kim, S. Jeong, *J. Am. Chem. Soc.* **2013**, 135, 5278.
- [17] L. Lin, Z. Li, J. Feng, Z. Zhang, *Phys. Chem. Chem. Phys.* **2013**, 15, 6063.
- [18] T. Kim, J. H. Song, T. Park, S. Jeong, *ACS Energy Lett.* **2020**, 5, 248.
- [19] W. Shockley, H. J. Queisser, *J. Appl. Phys.* **1961**, 32, 510.
- [20] P. Reiss, M. Carrière, C. Lincheneau, L. Vaure, S. Tamang, *Chem. Rev.* **2016**, 116, 10731.
- [21] T. Rauch, M. Böberl, S. F. Tedde, J. Fürst, M. V. Kovalenko, G. Hesser, U. Lemmer, W. Heiss, O. Hayden, *Nat. Photonics* **2009**, 3, 332.
- [22] A. Karani, L. Yang, S. Bai, M. H. Futscher, H. J. Snaith, B. Ehrler, N. C. Greenham, D. Di, *ACS Energy Lett.* **2018**, 3, 869.
- [23] H. Hosokawa, R. Tamaki, T. Sawada, A. Okonogi, H. Sato, Y. Ogomi, S. Hayase, Y. Okada, T. Yano, *Nat. Commun.* **2019**, 10, 43.
- [24] R. Dalven, *Phys. Rev. B* **1973**, 8, 6033.
- [25] H. Lu, X. Meng, *Sci. Rep.* **2015**, 5, 16939.
- [26] R. Sun, P. Dong, N. Feng, C. Hong, J. Michel, M. Lipson, L. Kimerling, *Opt. Express* **2007**, 15, 17967.
- [27] F. W. Wise, *Acc. Chem. Res.* **2000**, 33, 773.
- [28] M. A. Hines, G. D. Scholes, *Adv. Mater.* **2003**, 15, 1844.
- [29] Y. Pan, Y. R. Li, Y. Zhao, D. L. Akins, *J. Chem. Educ.* **2015**, 92, 1860.
- [30] H. Choi, J. Kwan Kim, J. Hoon Song, Y. Kim, S. Jeong, *Appl. Phys. Lett.* **2013**, 102, 193902.
- [31] H. Aqoma, I. F. Imran, M. Al Mubarak, W. T. Hadmojo, Y. R. Do, S. Y. Jang, *Adv. Energy Mater.* **2020**, 10, 1903294.
- [32] T. Kim, Y. Gao, H. Hu, B. Yan, Z. Ning, L. K. Jagadamma, K. Zhao, A. R. Kirmani, J. Eid, M. M. Adachi, E. H. Sargent, P. M. Beaujuge, A. Amassian, *Nano Energy* **2015**, 17, 196.
- [33] Y. L. Li, P. N. Yeh, S. Sharma, S. A. Chen, *J. Mater. Chem. A* **2017**, 5, 21528.
- [34] G. Shi, Y. Wang, Z. Liu, L. Han, J. Liu, Y. Wang, K. Lu, S. Chen, X. Ling, Y. Li, S. Cheng, W. Ma, *Adv. Energy Mater.* **2017**, 7, 1602667.
- [35] T. Kim, Y. Firdaus, A. R. Kirmani, R. Z. Liang, H. Hu, M. Liu, A. El Labban, S. Hoogland, P. M. Beaujuge, E. H. Sargent, A. Amassian, *ACS Energy Lett.* **2018**, 3, 1307.
- [36] Y. Zhang, M. Gu, N. Li, Y. Xu, X. Ling, Y. Wang, S. Zhou, F. Li, F. Yang, K. Ji, J. Yuan, W. Ma, *J. Mater. Chem. A* **2018**, 6, 24693.
- [37] Y. Bi, S. Pradhan, M. Z. Akgul, S. Gupta, A. Stavrinadis, J. Wang, G. Konstantatos, *ACS Energy Lett.* **2018**, 3, 1753.
- [38] L. Hu, Y. Wang, S. B. Shivarudraiah, J. Yuan, X. Guan, X. Geng, A. Younis, Y. Hu, S. Huang, T. Wu, J. E. Halpert, *ACS Appl. Mater. Interfaces* **2020**, 12, 2313.
- [39] A. J. Gatesman, J. Waldman, M. Ji, C. Musante, S. Yngvesson, *IEEE Microw. Guid. Wave Lett.* **2000**, 10, 264.
- [40] P. Yu, J. Wu, S. Liu, J. Xiong, C. Jagadish, Z. M. Wang, *Nano Today* **2016**, 11, 704.
- [41] T. L. Chu, S. S. Chu, J. Britt, C. Ferekides, C. Wang, C. Q. Wu, H. S. Ullal, *IEEE Electron Device Lett.* **1992**, 13, 303.
- [42] C. P. Liu, C. L. Chuang, *Sol. Energy* **2012**, 86, 2795.
- [43] M. M. Tavakoli, K. H. Tsui, Q. Zhang, J. He, Y. Yao, D. Li, Z. Fan, *ACS Nano* **2015**, 9, 10287.
- [44] W. Groh, A. Zimmermann, *Macromolecules* **1991**, 24, 6660.
- [45] M. B. Price, J. Butkus, T. C. Jellicoe, A. Sadhanala, A. Briane, J. E. Halpert, K. Broch, J. M. Hodgkiss, R. H. Friend, F. Deschler, *Nat. Commun.* **2015**, 6, 8420.
- [46] D. T. F. Marple, *J. Appl. Phys.* **1964**, 35, 539.
- [47] Z. J. Li-Kao, N. Naghavi, F. Erfurth, J. F. Guillemoles, I. Gérard, A. Etcheberry, J. L. Pelouard, S. Collin, G. Voorwinden, D. Lincot, *Prog. Photovoltaics Res. Appl.* **2012**, 20, 582.
- [48] N. M. Ravindra, P. Ganapathy, J. Choi, *Infrared Phys. Technol.* **2007**, 50, 21.
- [49] C. Cho, J. H. Song, C. Kim, S. Jeong, J. Y. Lee, *Sci. Rep.* **2017**, 7, 1.
- [50] X. Zhang, C. Hägglund, E. M. J. Johansson, *Energy Environ. Sci.* **2017**, 10, 216.
- [51] A. J. Labelle, S. M. Thon, S. Masala, M. M. Adachi, H. Dong, M. Farhani, A. H. Ip, A. Fratallocchi, E. H. Sargent, *Nano Lett.* **2015**, 15, 1101.
- [52] R. Tena-Zaera, J. Elias, C. Lvy-Clement, *Appl. Phys. Lett.* **2008**, 93, 233119.
- [53] O. L. Muskens, J. G. Rivas, R. E. Algra, E. P. A. M. Bakkers, A. Lagendijk, *Nano Lett.* **2008**, 8, 2638.
- [54] Q. Zhang, G. Cao, *Nano Today* **2011**, 6, 91.
- [55] H. Wang, T. Kubo, J. Nakazaki, T. Kinoshita, H. Segawa, *J. Phys. Chem. Lett.* **2013**, 4, 2455.
- [56] S. Chen, Y. Jie Wang, Q. Liu, G. Shi, Z. Liu, K. Lu, L. Han, X. Ling, H. Zhang, S. Cheng, W. Ma, *Adv. Energy Mater.* **2018**, 8, 1701194.
- [57] S. W. Baek, J. H. Song, W. Choi, H. Song, S. Jeong, J. Y. Lee, *Adv. Mater.* **2015**, 27, 8102.
- [58] A. H. Proppe, J. Xu, R. P. Sabatini, J. Z. Fan, B. Sun, S. Hoogland, S. O. Kelley, O. Voznyy, E. H. Sargent, *Nano Lett.* **2018**, 18, 7052.
- [59] Y. Liu, M. Gibbs, J. Puthusser, S. Gaik, R. Ihly, H. W. Hillhouse, M. Law, *Nano Lett.* **2010**, 10, 1960.
- [60] N. Y. Morgan, C. A. Leatherdale, M. Drndić, M. V. Jarosz, M. A. Kastner, M. Bawendi, *Phys. Rev. B – Condens. Matter Mater. Phys.* **2002**, 66, 075339.
- [61] J. M. Luther, M. Law, Q. Song, C. L. Perkins, M. C. Beard, A. J. Nozik, *ACS Nano* **2008**, 2, 271.

- [62] J. Tang, K. W. Kemp, S. Hoogland, K. S. Jeong, H. Liu, L. Levina, M. Furukawa, X. Wang, R. Debnath, D. Cha, K. W. Chou, A. Fischer, A. Amassian, J. B. Asbury, E. H. Sargent, *Nat. Mater.* **2011**, *10*, 765.
- [63] J. Xu, O. Voznyy, M. Liu, A. R. Kirmani, G. Walters, R. Munir, M. Abdelsamie, A. H. Proppe, A. Sarkar, F. P. García De Arquer, M. Wei, B. Sun, M. Liu, O. Ouellette, R. Quintero-Bermudez, J. Li, J. Fan, L. Quan, P. Todorovic, H. Tan, S. Hoogland, S. O. Kelley, M. Stefiak, A. Amassian, E. H. Sargent, *Nat. Nanotechnol.* **2018**, *13*, 456.
- [64] L. Hu, X. Geng, S. Singh, J. Shi, Y. Hu, S. Li, X. Guan, T. He, X. Li, Z. Cheng, R. Patterson, S. Huang, T. Wu, *Nano Energy* **2019**, *64*, 103922.
- [65] M. Gu, Y. Wang, F. Yang, K. Lu, Y. Xue, T. Wu, H. Fang, S. Zhou, Y. Zhang, X. Ling, Y. Xu, F. Li, J. Yuan, M. A. Loi, Z. Liu, W. Ma, *J. Mater. Chem. A* **2019**, *7*, 15951.
- [66] X. D. Mai, H. J. An, J. H. Song, J. Jang, S. Kim, S. Jeong, *J. Mater. Chem. A* **2014**, *2*, 20799.
- [67] A. Stavrinadis, G. Konstantatos, *ChemPhysChem* **2016**, *17*, 632.
- [68] Y. Zhang, D. Zherebetskyy, N. D. Bronstein, S. Barja, L. Lichtenstein, A. P. Alivisatos, L. W. Wang, M. Salmeron, *ACS Nano* **2015**, *9*, 10445.
- [69] H. Tavakoli Dastjerdi, R. Tavakoli, P. Yadav, D. Prochowicz, M. Saliba, M. M. Tavakoli, *ACS Appl. Mater. Interfaces* **2019**, *11*, 26047.
- [70] C. H. M. Chuang, P. R. Brown, V. Bulović, M. G. Bawendi, *Nat. Mater.* **2014**, *13*, 796.
- [71] L. Hu, Z. Zhang, R. J. Patterson, Y. Hu, W. Chen, C. Chen, D. Li, C. Hu, C. Ge, Z. Chen, L. Yuan, C. Yan, N. Song, Z. L. Teh, G. J. Conibeer, J. Tang, S. Huang, *Nano Energy* **2018**, *46*, 212.
- [72] M. J. Choi, F. P. García de Arquer, A. H. Proppe, A. Seifitokaldani, J. Choi, J. Kim, S. W. Baek, M. Liu, B. Sun, M. Biondi, B. Scheffell, G. Walters, D. H. Nam, J. W. Jo, O. Ouellette, O. Voznyy, S. Hoogland, S. O. Kelley, Y. S. Jung, E. H. Sargent, *Nat. Commun.* **2020**, *11*, 103.
- [73] Z. Ning, X. Gong, R. Comin, G. Walters, F. Fan, O. Voznyy, E. Yassitepe, A. Buin, S. Hoogland, E. H. Sargent, *Nature* **2015**, *523*, 324.
- [74] B. Sun, A. Johnston, C. Xu, M. Wei, Z. Huang, Z. Jiang, H. Zhou, Y. Gao, Y. Dong, O. Ouellette, X. Zheng, J. Liu, M. J. Choi, Y. Gao, S. W. Baek, F. Laquai, O. M. Bakr, D. Ban, O. Voznyy, F. P. García de Arquer, E. H. Sargent, *Joule* **2020**, *4*, 1542.
- [75] A. H. Ip, S. M. Thon, S. Hoogland, O. Voznyy, D. Zhitomirsky, R. Debnath, L. Levina, L. R. Rollny, G. H. Carey, A. Fischer, K. W. Kemp, I. J. Kramer, Z. Ning, A. J. Labelle, K. W. Chou, A. Amassian, E. H. Sargent, *Nat. Nanotechnol.* **2012**, *7*, 577.
- [76] M. Liu, O. Voznyy, R. Sabatini, F. P. García De Arquer, R. Munir, A. H. Balawi, X. Lan, F. Fan, G. Walters, A. R. Kirmani, S. Hoogland, F. Laquai, A. Amassian, E. H. Sargent, *Nat. Mater.* **2017**, *16*, 258.
- [77] Z. Ning, H. Dong, Q. Zhang, O. Voznyy, E. H. Sargent, *ACS Nano* **2014**, *8*, 10321.
- [78] G. H. Carey, I. J. Kramer, P. Kanjanaboos, G. Moreno-Bautista, O. Voznyy, L. Rollny, J. A. Tang, S. Hoogland, E. H. Sargent, *ACS Nano* **2014**, *8*, 11763.
- [79] D. Zherebetskyy, M. Scheele, Y. Zhang, N. Bronstein, C. Thompson, D. Britt, M. Salmeron, P. Alivisatos, L. W. Wang, *Science* **2014**, *344*, 1380.
- [80] Y. Cao, A. Stavrinadis, T. Lasanta, D. So, G. Konstantatos, *Nat. Energy* **2016**, *1*, 16035.
- [81] A. Hassinen, I. Moreels, K. De Nolf, P. F. Smet, J. C. Martins, Z. Hens, *J. Am. Chem. Soc.* **2012**, *134*, 20705.
- [82] N. C. Anderson, M. P. Hendricks, J. J. Choi, J. S. Owen, *J. Am. Chem. Soc.* **2013**, *135*, 18536.
- [83] A. Stavrinadis, S. Pradhan, P. Papagiorgis, G. Itkos, G. Konstantatos, *ACS Energy Lett.* **2017**, *2*, 739.
- [84] L. C. Cass, M. Malicki, E. A. Weiss, *Anal. Chem.* **2013**, *85*, 6974.
- [85] H. Aqoma, M. Al Mubarak, W. T. Hadmojo, E. H. Lee, T. W. Kim, T. K. Ahn, S. H. Oh, S. Y. Jang, *Adv. Mater.* **2017**, *29*, 1605756.
- [86] D. M. Kroupa, M. Vörös, N. P. Brawand, B. W. McNichols, E. M. Miller, J. Gu, A. J. Nozik, A. Sellinger, G. Galli, M. C. Beard, *Nat. Commun.* **2017**, *8*, 15257.
- [87] P. R. Brown, D. Kim, R. R. Lunt, N. Zhao, M. G. Bawendi, J. C. Grossman, V. Bulović, *ACS Nano* **2014**, *8*, 5863.
- [88] M. Yuan, D. Zhitomirsky, V. Adinolfi, O. Voznyy, K. W. Kemp, Z. Ning, X. Lan, J. Xu, J. Y. Kim, H. Dong, E. H. Sargent, *Adv. Mater.* **2013**, *25*, 5586.
- [89] Y. Gao, J. Zheng, W. Chen, L. Yuan, Z. L. Teh, J. Yang, X. Cui, G. Conibeer, R. Patterson, S. Huang, *J. Phys. Chem. Lett.* **2019**, *10*, 5729.
- [90] Y. Zhang, J. He, P. N. Wang, J. Y. Chen, Z. J. Lu, D. R. Lu, J. Guo, C. C. Wang, W. L. Yang, *J. Am. Chem. Soc.* **2006**, *128*, 13396.
- [91] H. Liu, Q. Dong, R. Lopez, *Nanomaterials* **2018**, *8*, 341.
- [92] S. Kim, A. R. Marshall, D. M. Kroupa, E. M. Miller, J. M. Luther, S. Jeong, M. C. Beard, *ACS Nano* **2015**, *9*, 8157.
- [93] Y. Wang, K. Lu, L. Han, Z. Liu, G. Shi, H. Fang, S. Chen, T. Wu, F. Yang, M. Gu, S. Zhou, X. Ling, X. Tang, J. Zheng, M. A. Loi, W. Ma, *Adv. Mater.* **2018**, *30*, 1704871.
- [94] J. Zhang, J. Gao, E. M. Miller, J. M. Luther, M. C. Beard, *ACS Nano* **2014**, *8*, 614.
- [95] J. Y. Woo, S. Lee, S. Lee, W. D. Kim, K. Lee, K. Kim, H. J. An, D. C. Lee, S. Jeong, *J. Am. Chem. Soc.* **2016**, *138*, 876.
- [96] Z. Ning, O. Voznyy, J. Pan, S. Hoogland, V. Adinolfi, J. Xu, M. Li, A. R. Kirmani, J. P. Sun, J. Minor, K. W. Kemp, H. Dong, L. Rollny, A. Labelle, G. Carey, B. Sutherland, I. Hill, A. Amassian, H. Liu, J. Tang, O. M. Bakr, E. H. Sargent, *Nat. Mater.* **2014**, *13*, 822.
- [97] J. Y. Woo, J. H. Ko, J. H. Song, K. Kim, H. Choi, Y. H. Kim, D. C. Lee, S. Jeong, *J. Am. Chem. Soc.* **2014**, *136*, 8883.
- [98] J. Choi, M. J. Choi, J. Kim, F. Dinic, P. Todorovic, B. Sun, M. Wei, S. W. Baek, S. Hoogland, F. P. García de Arquer, O. Voznyy, E. H. Sargent, *Adv. Mater.* **2020**, *32*, 1906497.
- [99] J. Tang, X. Wang, L. Brzozowski, D. A. R. A. Barkhouse, R. Debnath, L. Levina, E. H. Sargent, *Adv. Mater.* **2010**, *22*, 1398.
- [100] M. J. Choi, J. Oh, J. K. Yoo, J. Choi, D. M. Sim, Y. S. Jung, *Energy Environ. Sci.* **2014**, *7*, 3052.
- [101] B. Martín-García, Y. Bi, M. Prato, D. Spirito, R. Krahne, G. Konstantatos, I. Moreels, *Sol. Energy Mater. Sol. Cells* **2018**, *183*, 1.
- [102] Z. Jin, M. Yuan, H. Li, H. Yang, Q. Zhou, H. Liu, X. Lan, M. Liu, J. Wang, E. H. Sargent, Y. Li, *Adv. Funct. Mater.* **2016**, *26*, 5284.
- [103] S. W. Baek, S. H. Lee, J. H. Song, C. Kim, Y. S. Ha, H. Shin, H. Kim, S. Jeong, J. Y. Lee, *Energy Environ. Sci.* **2018**, *11*, 2078.
- [104] H. Choi, S. Jeong, *Int. J. Precis. Eng. Manuf. Green Technol.* **2018**, *5*, 349.
- [105] M. Z. Akgul, A. Figueroba, S. Pradhan, Y. Bi, G. Konstantatos, *ACS Photonics* **2020**, *7*, 588.
- [106] C. Chen, X. Qiu, S. Ji, C. Jia, C. Ye, *CrystEngComm* **2013**, *15*, 7644.
- [107] L. Hu, R. J. Patterson, Z. Zhang, Y. Hu, D. Li, Z. Chen, L. Yuan, Z. L. Teh, Y. Gao, G. J. Conibeer, S. Huang, *J. Mater. Chem. C* **2018**, *6*, 731.
- [108] J. T. Oh, H. Cho, S. Y. Bae, S. J. Lim, J. Kang, I. H. Jung, H. Choi, Y. Kim, *Int. J. Energy Res.* **2020**, *44*, 11006.
- [109] S. L. Diedenhofen, M. Bernechea, K. M. Felter, F. C. Grozema, L. D. A. Siebbeles, *Sol. RRL* **2019**, *3*, 1900075.
- [110] R. W. Crisp, F. S. M. Hashemi, J. Alkemade, N. Kirkwood, G. Grimaldi, S. Kinge, L. D. A. Siebbeles, J. R. van Ommen, A. J. Houtepen, *Adv. Mater. Interfaces* **2020**, *7*, 1901600.
- [111] R. W. Crisp, N. Kirkwood, G. Grimaldi, S. Kinge, L. D. A. Siebbeles, A. J. Houtepen, *ACS Appl. Energy Mater.* **2018**, *1*, 6569.
- [112] J. R. Heath, J. J. Shiang, *Chem. Soc. Rev.* **1998**, *27*, 65.

- [113] H. Fu, A. Zunger, *Phys. Rev. B – Condens. Matter Mater. Phys.* **1997**, 56, 1496.
- [114] Y. Kim, J. H. Chang, H. Choi, Y. H. Kim, W. K. Bae, S. Jeong, *Chem. Sci.* **2020**, 11, 913.
- [115] M. A. Green, E. D. Dunlop, J. Hohl-Ebinger, M. Yoshita, N. Kopidakis, X. Hao, *Prog. Photovoltaics Res. Appl.* **2020**, 28, 629.
- [116] O. Voznyy, L. Levina, F. Fan, G. Walters, J. Z. Fan, A. Kiani, A. H. Ip, S. M. Thon, A. H. Proppe, M. Liu, E. H. Sargent, *Nano Lett.* **2017**, 17, 7191.
- [117] J. Jean, T. S. Mahony, D. Bozyigit, M. Sponseller, J. Holovsky, M. G. Bawendi, V. Bulović, *ACS Energy Lett.* **2017**, 2, 2616.
- [118] O. Ouellette, A. Lesage-Landry, B. Scheffel, S. Hoogland, F. P. García de Arquer, E. H. Sargent, *Adv. Funct. Mater.* **2020**, 30, 1908200.
- [119] A. M. Ealias, M. P. Saravanakumar, in *IOP Conf. Series: Materials Science and Engineering*, Institute Of Physics Publishing, Bristol, UK **2017**.
- [120] P. Guyot-Sionnest, *J. Phys. Chem. Lett.* **2012**, 3, 1169.



Taewan Kim received his Ph.D. degree from the group of Taiho Park at POSTECH, South Korea, where he worked on both perovskite and quantum dot solar cells and developed optical and electrical device design for photoconversion. In 2020, he joined Sohee Jeong's group, where he is studying quantum dot synthesis and optoelectronic device fabrication.



Taiho Park is a professor in the Department of Chemical Engineering at POSTECH, South Korea, since 2007. Prof. Park received his Ph.D. from the University of Cambridge, UK, under the supervision of Prof. Andrew B. Holmes; then worked as a post-doctoral researcher under Prof. Steven C. Zimmerman at the University of Illinois (Urbana-Champaign), USA. Current research interests include the material properties and device functions of optoelectronic devices.



Jongmin Choi is an assistant professor in the Department of Energy Science & Engineering at DGIST, Daegu, Korea. He received his B.S. and Ph.D. degrees from the Department of Chemical Engineering at POSTECH in 2010 and 2016, respectively, under the supervision of Prof. Taiho Park. After that, he carried out his postdoctoral research in Edward H. Sargent research group at the University of Toronto, Canada, from 2016 to 2018. His research focuses on the developments of next-generation optoelectronic materials and devices.